

DIRECT AND INDIRECT THERMOSPHERIC HEATING SOURCES FOR SOLAR CYCLES 21–23

D. J. KNIPP¹, W. K. TOBISKA² and B. A. EMERY³

¹*Department of Physics, US Air Force Academy, CO 80840, USA*

(e-mail: delores.knipp@usafa.af.mil)

²*Space Environment Technologies, Pacific Palisades, CA 90272, USA*

(e-mail: ktobiska@spacenvironment.net)

³*High Altitude Observatory, NCAR, Boulder, CO 80301, USA*

(e-mail: emery@ucar.edu)

(Received 3 September 2004; accepted 14 October 2004)

Abstract. Solar variability is often cast in terms of radiative emission and the associated long-term climate response; however, growing societal reliance on technology is creating more interest in *day-to-day* solar variability. This variability is associated with both solar radiative and solar wind emissions. In this paper we explore the combined effects of radiative and solar wind fluctuations at Earth. The fluctuations in radiative and geomagnetic power create an extended interval of solar maximum for the upper atmosphere. We use a trio of empirical models to estimate, over the last three solar cycles, the relative contributions of solar extreme ultraviolet (UV) power, Joule power, and particle kinetic power to the Earth's upper atmosphere energy budget. Daily power values are derived from three source models. The SOLAR2000 solar irradiance specification model provides estimates of the daily extreme and far UV solar power input. Geomagnetic power is derived from a combination of satellite-estimated particle precipitation power and an empirical model of Joule power from hemispherically integrated estimates of high-latitude energy deposition. During the interval 1975 to 2003, the average daily contributions were: particles – 36 GW, Joule-95 GW and solar-464 GW for a total of 595 GW. Solar wind-driven geomagnetic power provided 22% of the total global upper atmospheric energy. In the top 15 power events, geomagnetic power contributed two-thirds of the total power budget. In each of these events, Joule power alone exceeded solar power. With rising activity, Joule power becomes the most variable element of solar upper atmosphere interactions.

1. Introduction

The Sun is the primary heating agent for the upper atmosphere. Solar input controls the basic structure and composition of the thermosphere. Temporal and spatial variations of solar power produce temperature changes that drive local and global circulations via the pressure gradient force. On a practical level the temperature changes create density perturbations that strongly influence the dynamics of orbiting bodies in the Earth's atmosphere. This paper provides an accounting of the range and variability of three key sources of atmospheric energy over the last three solar cycles: solar radiation, Joule dissipation, and kinetic energy deposition by low-energy particles (primarily electrons). Figure 1 shows the two primary regions of concern: the dayside where solar EUV radiation dominates, and one of the two auroral zones where particle precipitation and Joule dissipation dominate.



Solar Physics xxx: 1–11, 2004.

© 2004 Kluwer Academic Publishers. Printed in the Netherlands.

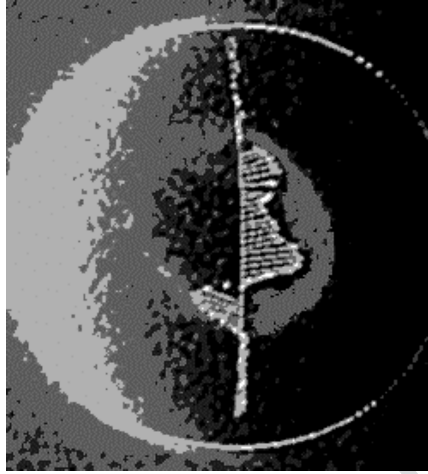


Figure 1. A view from the Dynamics Explorer (DE) 1 spacecraft showing solar radiative interaction on the dayside and glow from the northern auroral oval in the center. The arrows on the image indicate the thermospheric neutral winds created through solar wind – magnetosphere – thermosphere interactions. Neutral wind data were obtained with the DE-2 Fabry-Perot interferometer (after Killeen *et al.*, 1988).

The vast majority of radiation incident upon the top of the atmosphere originates as blackbody radiation from the low solar atmosphere in the wavelength range 10^0 – 10^6 nm. The direct power input to the Earth is roughly constant at 1366 Wm^{-2} . This energy passes through much of the atmosphere unimpeded, heats the Earth's surface, and drives weather and climate processes in the troposphere. There is, however, a small non-thermal component of solar radiation that interacts strongly with the Earth's upper atmosphere. The emissions from the solar upper atmosphere, mostly from the chromosphere and corona, are highly variable across the wavelengths 10^0 – 10^2 nm. The variations are present on day-to-day and solar cycle time frames. On an average, solar extreme ultraviolet (EUV) radiation, with a flux of approximately 2 mWm^{-2} , is the single largest contributor to the upper atmospheric heating budget.

The Sun also creates an indirect source of upper atmospheric energy deposition that is highly variable. Approximately 60% of the energy deposited in the magnetosphere by the solar wind is ultimately dissipated in Earth's ionosphere – thermosphere – mesosphere system (Lu *et al.*, 1998). During some geomagnetic storms, this value rises to over 80% (Knipp *et al.*, 1998). The indirect dissipation takes place in two primary ways: Joule power dissipation and low-energy particle deposition in the auroral zones. The sum of these, which we call geomagnetic power, contributes roughly 20% of the power budget but in extreme events can contribute more than two-thirds of the budget. Relatively speaking, the Joule power dissipation is the most variable of all of the inputs.

2. Background and Methodology

2.1. DAYSIDE POWER

Because solar spectral irradiances are the foundation for understanding scattering and photo-absorption processes in atmospheres and ionospheres, significant effort has been devoted to specifying the solar spectrum and its interaction with the Earth (Fröhlich and Lean, 1998; Woods *et al.*, 2004, and references therein). Tobiska *et al.* (2000) and Tobiska and Bouwer (in press) developed a model of the full solar spectrum called SOLAR2000. The model is an empirical solar irradiance specification tool for characterizing solar irradiance variability across the solar spectrum (10^0 – 10^6 nm). It uses the solar irradiance proxy inputs of F10.7 for coronal emission and the Magnesium II (Mg II) core-to-wing ratio for chromospheric emission. Thermospherically effective irradiances are modeled at 1 nm resolution between 1 and 120 nm and reported in units of W m^{-2} at one astronomical unit. Consistent with the variations in solar EUV output, the magnitude of heating in all altitudes above 100 km changes substantially with solar activity. Daily estimates of power can be made for the interval from 1947 through 2003, with the more reliable values available after 1976.

Recent modifications to the SOLAR2000 include improved variability from the XUV–EUV through the FUV and UV (1–420 nm) wavelengths and a proxy-driven H I Lyman-alpha spectral irradiance at 121 nm. Additionally, the thermosphere ionosphere mesosphere energetics and dynamics solar EUV experiment (SEE) data (Woods *et al.*, 2000) are a part of the derivation of SOLAR2000 EUV between 1 and 120 nm. The SEE data includes 0.1–34 and 27–194 nm detector data. All satellite, rocket, and reference continua datasets used in the model derivation are now scaled to the absolute level of the SEE data in each ~ 0.1 nm wavelength bins (Tobiska and Bouwer, in press). Figure 2 shows the range of the SOLAR2000 model.

2.2. AURORAL ZONE POWER

Instruments onboard the NOAA TIROS and polar-orbiting operational environmental satellite (POES) and the defense meteorological satellite program (DMSP) satellites continually monitor the power flux carried by the protons and electrons that produce aurora in the atmosphere. TIROS observations began in late-1978. DMSP observations are available since 1983. Originally precipitating electrons in the range 300 eV to 20 keV were observed by TIROS sensors. Current POES observations cover the range from 50 eV to 20 keV, and DMSP sensors provide data in the range 30 eV to 30 keV. Energy from particles outside this range is minimal due to their small energy flux into the atmosphere (Hardy, Gussenhoven and Brautigam, 1989). Fuller-Rowell and Evans (1987) developed a technique that uses the electron-only or electron-plus-proton power flux observations obtained during a single pass of the satellite over a polar region (which takes about 25 min)

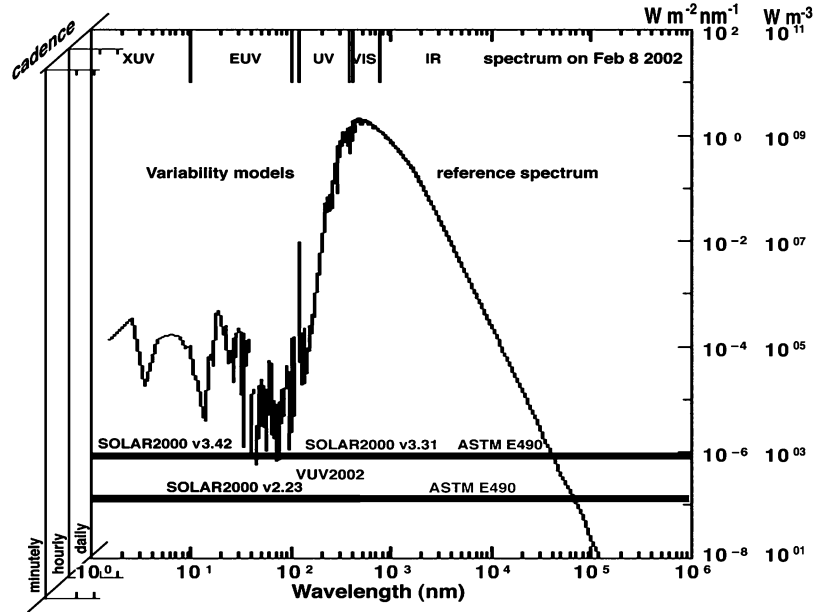


Figure 2. Combined model spectral coverage from SOLAR2000 EUV, UV, and ASTM-E490 reference spectra (ASTM-E490: <http://rredc.nrel.gov/solar/spectra/am0/references.html>).

to estimate the total power deposited in an entire polar region by the 50 eV to 20 keV particles. DMSP observations do not include protons. Hemispheric proton precipitation provides only a small increment ($\sim 12\%$) to the total deposited particle power estimated from NOAA satellites (Hubert *et al.*, 2002), so we regard their absence in the DMSP data as minimally important. Inter-calibration of data from all years and all instruments produced a composite particle dataset from NOAA and DMSP for each hemisphere that we summed over both hemispheres for the interval late-1978 through 2003 to create daily estimates of the particle precipitating power.

Joule power is closely associated with the level of geomagnetic activity. Chun *et al.* (1999) estimated hemispheric Joule heating with a quadratic fit to the northern Polar Cap (PC) index. The PC index is a ground magnetic measure of the strength and orientation of the overhead ionospheric current in the polar cap. It is used as a proxy for the electric field imposed on the polar ionosphere by the solar wind (Troshichev *et al.*, 1988). Chun *et al.* (1999) assembled a set of 12,000 hemispherically integrated Joule heating values derived from the assimilative mapping of ionospheric electrodynamics (AMIE) mapping procedure (Richmond and Kamide, 1988) as a statistical ensemble for binning Joule power against geomagnetic activity. Noting that the model underestimated Joule heating during strong storms, Knipp *et al.* (in press) included another fit parameter to improve the Joule power estimates. Using a series of multiple linear regression fits, they determined that the

TABLE 1
Fit coefficients for Joule power (from Knipp *et al.*, 2004)

Season	Month	Fit using absolute values of PC and Dst	R^2
Annual	January–December	$JH(GW) = 24.89 \times PC + 3.41 \times PC^2 + 0.41 \times Dst + .0015 \times Dst^2$	0.76
Winter	21 October–20 February	$JH(GW) = 13.36 \times PC + 5.08 \times PC^2 + 0.47 \times Dst + .0011 \times Dst^2$	0.84
Summer	21 April–20 August	$JH(GW) = 29.27 \times PC + 8.18 \times PC^2 - 0.04 \times Dst + .0126 \times Dst^2$	0.78
Equinox	21 February–20 April; 21 August–20 October	$JH(GW) = 29.14 \times PC + 2.54 \times PC^2 + 0.21 \times Dst + .0023 \times Dst^2$	0.74

Joule heating could be better parameterized using PC index *and* the disturbance storm time (Dst) index. In addition to goodness-of-fit they chose the regression parameters, PC and Dst, based on: (1) association with geomagnetic activity; (2) hourly cadence; and (3) relatively long-term, uninterrupted availability. Dst is a geomagnetic index measured by low-latitude stations. It can be thought of as a proxy for the electrical interaction of the nightside magnetosphere and ionosphere. As shown in Table I, Joule power is dependent on quadratic fits to both PC and Dst. The variations in seasonal coefficients are, in part, due to seasonal changes in conductivity in the auroral zones. We apply the seasonal coefficients to derive the Joule power presented in this paper.

A comparison of AMIE-derived Joule power and the model empirical results (Figure 3) indicate that the PC–Dst combination can provide a good proxy for simple, hemispheric-scale Joule power. We do not account for neutral wind effects that may contribute negatively to the energy budget when the ion flows are significantly different from neutral wind motions. Neither do we account for small-scale variability of the electric field which may add considerably to the Joule power. On balance, our geomagnetic power estimates are probably conservative.

3. Results

Using the models described above, we calculate the daily power input to the upper atmosphere from 1975 to 2003 (10,590 days). The upper gray curve in Figure 4 shows the daily solar short-wave power from the SOLAR2000 model. Average solar power input to the upper atmosphere is 464 ± 135 GW with a range from 285 GW in 1995 to 962 GW in 1989. The largest values of solar power occurred in the early years of solar cycles 21 and 22. The overall form of the solar cycle is clear, with the magnitude and variability of short-wave solar power rising dramatically during solar maximum.

The bottom gray curve of Figure 4 shows the low-energy precipitating particle power. We summed the daily contribution from both hemispheres. In order to

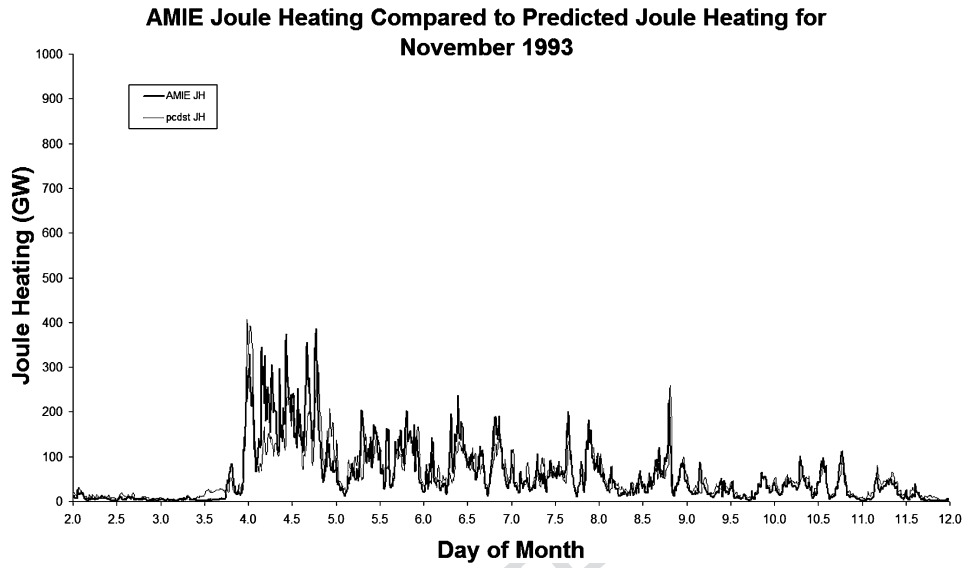


Figure 3. Joule power derived from the AMIE procedure compared to the proxy Joule heating values derived from the least squares fit to the ground magnetic indices shown in Table I.

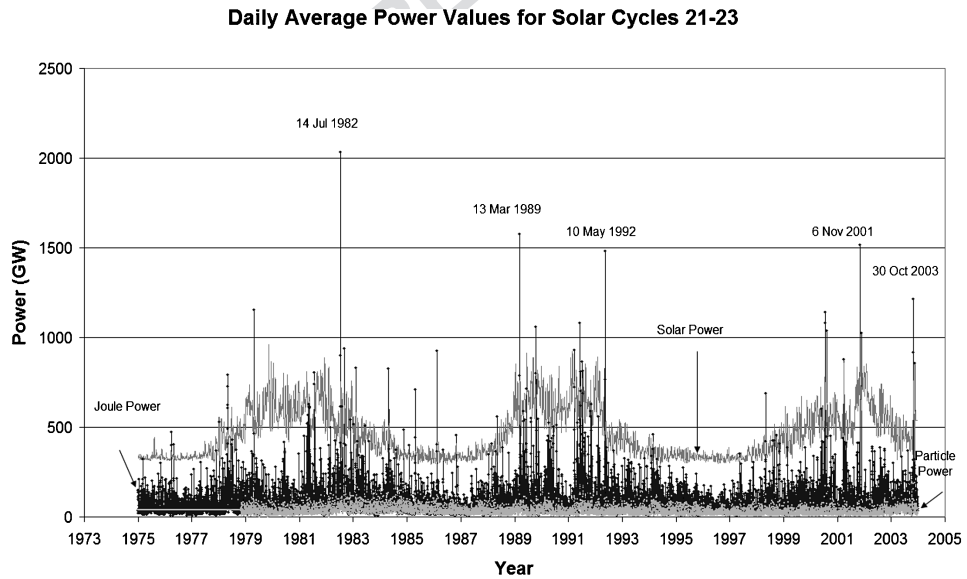


Figure 4. Particle power, Joule power, and solar power from 1975 to 2003.

make a reasonable comparison of total power for the interval 1975 to late-1978 150
 when particle power data were unavailable, we included the average value of the 151
 precipitating particle power, 36 GW. This is shown as the straight line in Figure 4. 152
 Overall, the particles contribute only a small fraction (6%) of the total power to 153

the upper atmosphere. On an average the precipitating electrons produce 36 ± 24 GW with a range from 11 GW in each of the solar minima to 290 GW in March 1989. Neither the average nor the standard deviation of the particle power varies significantly over the solar cycle.

The middle, black curve in Figure 4, with its sharp spikes, shows Joule power delivered to the upper atmosphere. This estimate is made by doubling the northern hemisphere value of Joule power. (Reliable estimates of Joule power from the southern hemisphere cannot be calculated for our interval because of breaks in the southern PC index data record.) Across the three solar cycles the daily average Joule power input to the upper atmosphere is 95 ± 93 GW. The daily Joule power ranges from 7 GW in 1997 to 2035 GW in 1982. Although the most extreme values of Joule power tend to occur during solar maximum years, significant Joule heating events with daily power in excess of 500 GW occur even during solar minimum years. Average values vary by 45% over the course of the solar cycle. The delineation between solar maximum and solar minimum tends to blur because the rising and declining phases of the solar cycle have broad shoulders with significant Joule power delivered during solar wind-driven geomagnetic storms.

Table II summarizes the average power estimates and standard deviations over all of the solar cycles and over solar minimum and solar maximum years. During solar minimum years Joule power contributes 16% of the power input and much of the variability in total power. During solar maximum years Joule power contributes 16% of the power input and an even larger fraction of the variability. The bottom two rows of Table II present the statistics for the top 5% and the top 1% of the power input events. In the top 1% of days the solar power was 50% above average and the particle power was roughly 200% above average. The Joule power increased by a factor of six.

Figure 5 shows the temporal variation of the total power. The average total power input is 595 ± 190 GW. The minimum value of 525 GW occurred in 1977, and the

TABLE II
Summary of average power and variability

Power category		Particle (GW)	Joule (GW)	Solar (GW)	Total (GW)
Solar min: 75–77, 83–87, 93–98	Average S.D.	38 (8%) 21	77 (16%) 63	359 (76%) 46	474 (101)
Solar cycles 21–23	Average S.D.	36 (6%) 24	95 (16%) 93	464 (78%) 135	596 (190)
Solar max: 78–82, 88–92, 99–03	Average S.D.	35 (5%) 23	112 (16%) 111	562 (79%) 116	710 (182)
Top 5% of power events	Average S.D.	73 (7%) 36	331 (30%) 226	687 (63%) 116	1090 (226)
Top 1% of power events	Average S.D.	104 (7%) 44	638 (45%) 306	691 (48%) 113	1433 (313)

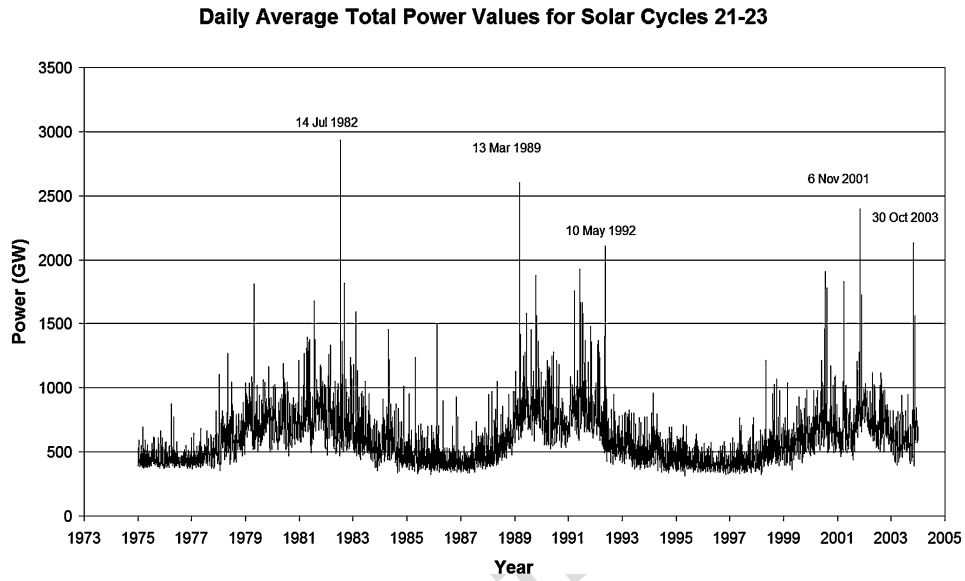


Figure 5. Total power from 1975 to 2003 (note scale change from Figure 4).

maximum value of 2932 GW occurred in 1982. The top 1% of all heating events occurred exclusively during solar maximum years. These events had substantial contributions from Joule power ($\sim 45\%$).

For the 15 most extreme events (listed in Table III) geomagnetic heating constituted approximately 65% of the power budget. These extraordinary events are defined roughly by the following conditions: total Joule power exceeding 1200 GW and particle power exceeding 160 GW. In all of these events, Joule power alone exceeded the solar EUV power. In our entire dataset, Joule power alone exceeded solar power in over 60 events. The dates of the top five daily heating events (of $\sim 10,590$ days) are specifically labeled in Figures 4 and 5. Among these dates are the notorious March 1989 and October 2003 storms.

4. Discussion

The intricacies of analyzing and forecasting extreme upper atmospheric heating events have challenged scientists and those with operational interests in the near space environment for years. For average, global-scale estimates, the geomagnetic power extracted from solar wind-magnetosphere interactions plays a secondary role in powering the upper atmosphere. Extreme power deposition events are different. In those cases, Joule power equals or exceeds solar power input. Additionally, for these extreme events the solar energy deposition rates were already enhanced above background, so the upper atmosphere experiences an overabundance of power.

TABLE III
Top 15 daily power events

Year	Month/day	Particle Pwr (GW)	Joule Pwr (GW)	Solar Pwr (GW)	Total Pwr (GW)	Rank	% Joule Pwr	% Joule + particle Pwr
1979	25-April	152	1154	502	1808	13	64	72
1982	13-July	183	900	690	1772	15	51	61
1982	14-July	159	2035	739	2932	1	69	75
1982	6-September	267	941	609	1817	12	52	66
1989	13-March	290	1576	732	2599	2	61	72
1989	21-October	147	1059	668	1874	8	56	64
1991	5-June	126	1082	717	1924	6	56	63
1992	10-May	162	1484	459	2105	5	71	78
2000	15-July	173	1083	652	1909	7	57	66
2000	16-July	51	1144	676	1871	9	61	62
2000	12-August	129	1040	612	1781	14	58	66
2001	31-March	144	878	805	1826	11	48	64
2001	6-November	122	1518	754	2394	3	63	74
2003	29-October	185	918	760	1863	10	49	59
2003	30-October	156	1214	758	2128	4	57	64
	Average	163	1202	675	2038		59	67

202 The power sources are distributed around the globe in different ways, so that
 203 regional influences of these sources can result in any one of these terms dominat-
 204 ing the local energy balance. There are also differing distributions in altitude. For
 205 SOLAR2000 the thermospheric energy deposition is in the 150–200 km range for
 206 almost all levels of solar activity. Low-energy electron power is primarily deposited
 207 in the 100–120 km range (Fuller-Rowell and Evans, 1987). Joule power is predom-
 208 inantly input in the 110–140 km level (Thayer and Semeter, 2004). These altitude
 209 dependencies also control heating efficiencies.

210 Further exacerbating the situation is the issue of heating efficiency. In the case
 211 of auroral particles, the heating efficiency is roughly 50% (Rees *et al.*, 1983). The
 212 heating efficiency of solar EUV is altitude dependent, but averages to roughly 50%,
 213 as well (Torr, Torr and Richards, 1980). Joule power, however, transfers energy to
 214 the neutral atmosphere at nearly 100% efficiency (Thayer and Semeter, 2004). Thus,
 215 even moderately elevated Joule power values can compete with solar power as the
 216 dominant heating mechanism in the upper atmosphere.

217 Some events, such as the March 1989 and October 2003 storms, represent “per-
 218 fect storms.” Significant solar EUV bursts are followed by rapid, prolonged, and
 219 extreme solar wind interaction with the magnetosphere–ionosphere–thermosphere
 220 system. Extraordinary upper atmospheric heating results. This has important im-
 221 plications for processes such as satellite drag.

5. Summary

222

Using a trio of empirical models, we have quantified the relative roles of particle, 223
 Joule and solar EUV power. Solar power input is roughly 78% (464 GW) over the 224
 solar cycle. Particle kinetic power contributes approximately 6% (36 GW) of the 225
 upper atmosphere's energy across all phases of the solar cycle. On average, Joule 226
 power contributes 16% (95 GW) of the total power value but a much larger portion 227
 of the power variability. In the top 5% of heating events, geomagnetic (particle plus 228
 Joule) power provided $\sim 37\%$ of the total power and was the dominant contributor 229
 to the variability. In the top 15 events, geomagnetic power provided more than 230
 65% of the total power. This paper shows the relative importance of direct and 231
 indirect solar forcing of the Earth's upper atmosphere. Solar wind forcing competes 232
 with and at times exceeds solar radiative forcing; thereby adding a significant 233
 component of variability to the solar cycle impressed upon the upper atmosphere. 234
 When geomagnetic sources are accounted for, the peak upper atmospheric heating 235
 events are more extreme than those from solar EUV input only. Further, the solar 236
 maxima intervals expand to include broad shoulders of solar wind-driven heating 237
 from geomagnetic storms. 238

Acknowledgments

239

DJK and BAE were supported by National Science Foundation (NSF) Space 240
 Weather Grants 0077536 and 0208145, respectively. The northern PC data were 241
 provided by the Danish Meteorological Institute. The Dst Index was provided by 242
 WDC 2, Kyoto, Japan, and the NASA National Space Science Data Center. D. 243
 Evans (NOAA SEC) and F. Rich (AFRL/VX) provided the precipitating particle 244
 data. W. Xu (NCAR) processed the particle data. T. Welliver processed the Joule 245
 power regression data. 246

References

247

- Chun, F. *et al.*: 1999, *Geophys. Res. Lett.* **26**(8), 1101. 248
 Fröhlich, C. and Lean, J.: 1998, *Total Solar Irradiance Variations, International Astronomical Union* 249
Symposium 185: New Eyes to See Inside the Sun and Stars, Kluwer Academic Publishers, 250
 Dordrecht, The Netherlands, p. 89. 251
 Fuller-Rowell, T. J. and Evans, D. S.: 1987, *J. Geophys. Res.* **92**, 7606. 252
 Hardy, D. A., Gussenhoven, M. S. and Brautigam, D.: 1989, *J. Geophys. Res.* **94**, 370. 253
 Hubert, B. *et al.*: 2002, *J. Geophys. Res.* **107**, A11, doi: 10.1029/2002JA009205. 254
 Killeen, T. L. *et al.*: 1988, *J. Geophys. Res.* **93**, 2675. 255
 Knipp, D. J. *et al.*: 1998, *J. Geophys. Res.* **103**, 26197. 256
 Knipp, D. J. *et al.*: in press, *Adv. Space Res.* 257
 Lu, G. *et al.*: 1998, *J. Geophys. Res.* **103**, 11685. 258
 Rees, M. H., Emery, B., Roble, R., and Stamnes, K.: 1983, *J. Geophys. Res.* **88**, 6289. 259
 Richmond, A. D. and Kamide, Y.: 1988, *J. Geophys. Res.* **93**, 5741. 260

- 261 Thayer, J. P. and Semeter, J.: 2004, *J. Atmos. Solar Terr. Phys.* **66**, 807.
262 Tobiska, W. K., Woods, T. and Eparvier, F. *et al.*: 2000, *J. Atmos. Solar Terr. Phys.* **62**, 1233.
263 Tobiska, W. K. and Bouwer, S. D.: in press, *Adv. Space Res.*
264 Torr, M. R., Torr, D. G. and Richards, P. G.: 1980, *Geophys. Res. Lett.* **7**(5), 373.
265 Troshichev, O., Andersen, V. G., Vennerstrom, S., and Friis-Christensen, E.: 1988, *Planet. Space Sci.*
266 **36**, 1095.
267 Woods, T. N. *et al.*: 2000, *Phys. Chem. Earth* **25**(5–6), 393.
268 Woods, T. *et al.*: 2004, *Solar, AGU Monograph*, 10.1029/141GM11, p. 127.

UNCORRECTED PROOF